JARVIS, R. A. (1966). *J. Sci. Instrum.* **43**, 899–907.

KARLE, J. & HAUPTMAN, H. (1956). *Acta Cryst.* **9**, 635–651.

KARLE, I. L., HAUPTMAN, H., KARLE, J. & WING, A. B. (1958). *Acta Cryst.* **11**, 257–263.

KURKI-SUONIO, K. (1968). *Acta Cryst.* A**24**, 379–390.

MASLEN, E. N. (1967). *Acta Cryst.* **22**, 945–946.

O'CONNELL, A. M., RAE, A. I. M. & MASLEN, E. N. (1966). *Acta Cryst.* **21**, 208–219.

O'CONNOR, B. H. & MASLEN, E. N. (1973). *Acta Cryst.* To be published.

O'CONNOR, B. H. & MOORE, F. H. (1973). *Acta Cryst.* B**29**, 1903–1909.

O'CONNOR, B. H. & VALENTINE, T. M. (1969). *Acta Cryst.* B**25**, 2140–2144.

STEWART, R. F., DAVIDSON, E. R. & SIMPSON, W. T. (1965). *J. Chem. Phys.* **42**, 3175–3187.

Acta Cryst. (1973). B**29**, 1903

Neutron-Diffraction Refinement of the Crystal Structure of 1,3,5-Triacetylbenzene

BY B. H. O'CONNOR*

Department of Physics, University of Western Australia, Nedlands, Western Australia

AND F. H. MOORE

Australian Institute of Nuclear Science and Engineering, Lucas Heights, New South Wales, Australia

(*Received* 2 *April* 1973; *accepted* 29 *April* 1973)

A neutron-diffraction investigation of the crystal structure of 1,3,5-triacetylbenzene has been performed in parallel with an X-ray diffraction analysis, as part of a study of electron-density distribution. Data were collected with two crystals at a neutron wavelength of 1·192 Å, the total number of 1576 independent reflexions being limited to a maximum of 0·57 Å^{-1} in sin θ/λ. The positional and anisotropic thermal parameters were refined by block-diagonal least-squares calculations on $|F|^2$ with allowance for extinction effects in the data. The final model is discussed with reference to the intra- and intermolecular geometry and thermal motion.

Introduction

The present investigation (here abbreviated TABN) of the crystal structure of 1,3,5-triacetylbenzene (TAB) has been performed to complement the X-ray study (TABX) of TAB described in the accompanying paper by O'Connor (1973). Combined X-ray and neutron diffraction studies of organic molecules have been used, for example, by Coppens (1967), Coppens, Sabine, Delaplane & Ibers (1969) and Coppens & Vos (1971) to investigate the nature of the charge-density distribution in, respectively, *sym*-triazine, oxalic acid dihydrate and cyanuric acid. The advantage of using combined analyses for this purpose is that positional and thermal parameters obtained with neutron parameters can thus be employed with the X-ray data to construct Fourier difference maps which ideally reflect only the inadequacies of the spherical atom approximation (see TABX). If the expected bonding features are evident in the difference maps, it is then most useful to attempt a least-squares study of the valence-electron distribution, in which the positional and thermal parameters are fixed at the neutron values.

The details of molecular geometry and thermal motion are discussed in this paper rather than in the TABX account because of the general superiority of the neutron parameters.

Experimental

The sample of TAB which had been used to grow crystals for the TABX study was purified further by successive recrystallizations from acetone. It was then a simple matter to obtain crystals of sufficient volume for neutron diffraction by seeding a saturated solution of TAB in acetone. The crystals were all monoclinic prismatic with development of the {100}, {010} and {001} faces and were characterized by preferential growth normal to the unique axis. The intensity data were recorded with two crystals, the dimensions of which are given in Table 1. The smaller specimen (crystal 1) was used to measure the low-angle reflexions

Table 1. *Crystal dimensions*

Face indices	D*(Crystal 1)	D*(Crystal 2)
1 0 0 $\bar{1}$ 0 0	0·040 cm	0·120 cm
0 1 0 0 $\bar{1}$ 0	0·224	0·480
0 0 1 0 0 $\bar{1}$	0·470	0·762

* Length of normal between the specified pair of faces.

---

* Present address: Department of Physics, Western Australian Institute of Technology, South Bentley, Western Australia.

with the intention of reducing extinction effects and the larger specimen (crystal 2) was used for the high-angle reflexions in order to maintain an acceptable level of counting efficiency for the full range of data considered.

The intensity profiles were measured with a manual three-circle diffractometer situated at port 4H5 of the reactor HIFAR which is operated at Lucas Heights by the Australian Atomic Energy Commission. The incident neutron beam, obtained by reflexion from the (111) planes of a copper crystal monochromator, had a measured wavelength of 1·192 Å and a flux of approximately 5×10^5 neutrons $\text{cm}^{-2}\ \text{s}^{-1}$. The profiles were recorded by the $\theta/2\theta$-scan technique in the 'symmetric' instrument configuration, with the detector being stepped in increments of 3′ over a range of 5° divided equally between the peak and background segments of the profile. Careful analysis of the profile maxima showed that the $P2_1/c$ cell parameters from the TABX study [$a=8{\cdot}386$ (3), $b=16{\cdot}333$ (5), $c=7{\cdot}644$ (3) Å; $\beta=93{\cdot}69$ (3)°] were acceptable within the setting precision of the diffractometer circles. These cell parameters were adopted throughout the course of the TABN investigation.

468 acceptable reflexions were recorded with crystal 1 in the low-angle range of reciprocal space defined by the upper limit 0·420 Å^{-1} in $\sin\theta/\lambda$, and a further 1352 were recorded with crystal 2 in the range $0{\cdot}300\le\sin\theta/\lambda\le0{\cdot}570$. As the goniometer angles and initial detector position for the profile scan were set manually, it was necessary to devise checking procedures which indicated with reasonable certainty those reflexions that had been mis-set. It was not feasible, however, to assess the reliability of setting at the time of measurement. During the subsequent data-reduction stage, by which time the diffractometer was no longer available, 94 of the total 562 accessible in the low-angle range were rejected on the grounds that the angular settings were possibly in error. For the same reason 97 of the total 1213 accessible in the high-angle range were rejected. The list of 1352 acceptable high-angle data includes 244 reflexions also present in the set of low-angle data. These duplicate measurements were not averaged as part of a merge procedure as it could not be assumed that the extinction parameters for the two crystals would be identical. The structural least-squares refinement was therefore performed with two unscaled lists of data, the total number of independent observations for this purpose being 1576.

The reflexions 204 and $25\bar{2}$ were measured twice daily as standards during the data collection. Results showed that the counting system was effectively stable during the experiment. The intensity profiles were reduced to estimates of intensity by dividing each profile into peak and background sections such that the number of points in each section of background was the same, and together equalled the number of peak points. The intensity for P counts on the peak and B on the background is then

$$I=P-B\,.$$

The estimates of variance were determined with the approximation

$$\sigma^2(I)\simeq\sigma_1^2(I)+pI^2$$

where $\sigma_1^2(I)=P+B$ is the contribution from counting statistics. A reasonable estimate for p in the term pI^2, which is included to account for instrumental missetting errors, was not available at the data-reduction stage so that only the $\sigma_1^2(I)$ could be formed then. Absorption corrections were calculated according to the procedure of Busing & Levy (1957). The value of the linear absorption coefficient used in these calculations, 2·45 (10) cm^{-1}, was determined in a simple transmission experiment on crystal 2 with the detector mounted in the straight-through position. It is of interest that the experimental value for the absorption coefficient corresponds to a mean total scattering cross-section of 47 barns for hydrogen in TAB, compared with the value of 20·36 barns quoted by Melkonian (1949) for hydrogen in the free state. Note that the experimental proton scattering cross-sections (given by Melkonian for the neutron energy 0·058 eV used in the TAB determination) are 39, 42 and 44 barns for liquid state H_2O, n-butane and cetane, respectively.

The final lists of F_o^2 and $\sigma_1^2(F_o^2)$ for the two crystals are presented in Tables 2 and 3.

Table 2. *Observed structure factor squares* (*FOSQ*) *for crystal* 1 *with the estimated standard deviations* (*ESD*) *based on counting statistics*

Structure refinement

The model from the TABX analysis was refined by block-diagonal least-squares minimization of the quantity $\sum_i \sum_{\mathbf{H}} w_i(\mathbf{H}) \, . \, [F_{oi}^2(\mathbf{H}) - F_c^2(\mathbf{H}) y_i(\mathbf{H})/k_i]^2$ where $y_i(\mathbf{H})$ is the extinction factor for reflexions $\mathbf{H}$ in the ith data list. The mosaicity model adopted for the determination of y_i was the isotropic model described by Zachariasen (1969), in which the crystal is represented as an aggregate of perfect spherical domains of radius r_i with the misorientation of the domains following an isotropic Gaussian distribution of the form

$$W_i(\Delta) = \sqrt{2} g_i \exp(-2\pi g_i^2 \Delta^2) \, .$$

In this approximation the extinction factor is

$$y_i(\mathbf{H}) = [1 + 2Q_i(\mathbf{H}) T_i(\mathbf{H}) r_i^* / \lambda]^{-1/2} ;$$

where

$Q_i(\mathbf{H}) = F_c^2(\mathbf{H}) \lambda^3 / V_c^2 \sin 2\theta$ for neutron diffraction,

$T_i(\mathbf{H})$ is the mean path length for reflexion $\mathbf{H}$,

and

$$r_i^* = r_i / [1 + (r_i / \lambda g_i)^2]^{1/2}$$

is the extinction parameter to be refined in the least-squares calculation. The undefined symbols have their usual meaning.

In the block-diagonal calculation the following block structure was adopted: 9 × 9 matrices for each of the 27 atoms in the molecule (*i.e.* each atom was treated as anisotropic) and a 5 × 5 matrix for the parameters k_1, k_2, r_1^*, r_2^*, and the customary 'artificial' isotropic thermal parameter. The scattering lengths for carbon, oxygen and hydrogen were fixed at 6·61, 5·77 and $-3{\cdot}78f$ (Bacon, 1962), respectively. All reflexions were

Table 3. *Observed structure factor squares* (*FOSQ*) *for crystal* 2 *with the estimated standard deviations* (*ESD*) *based on counting statistics*

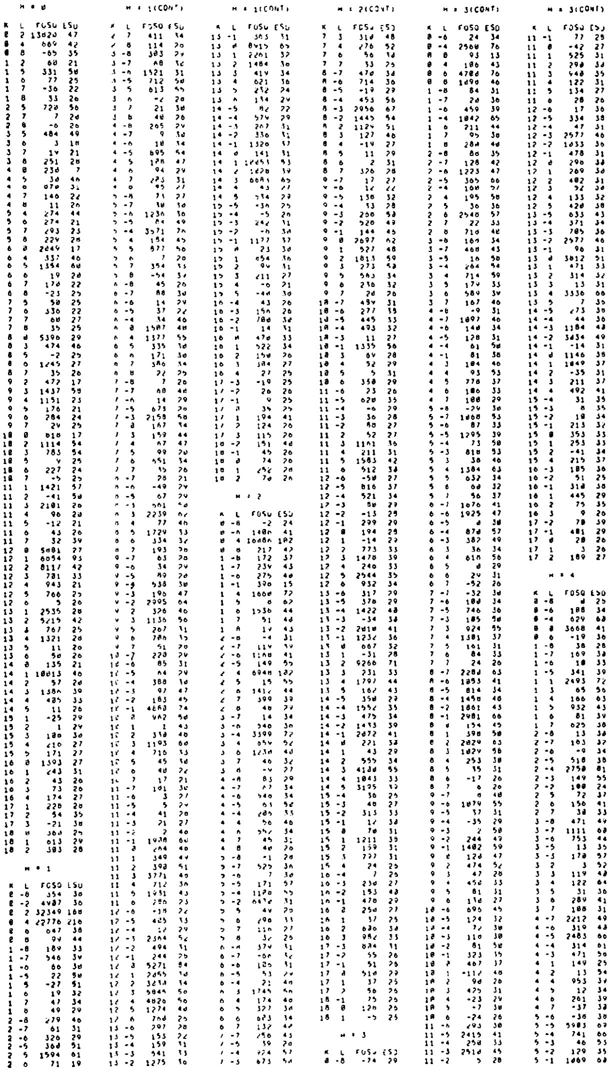

Table 3 (*cont.*)

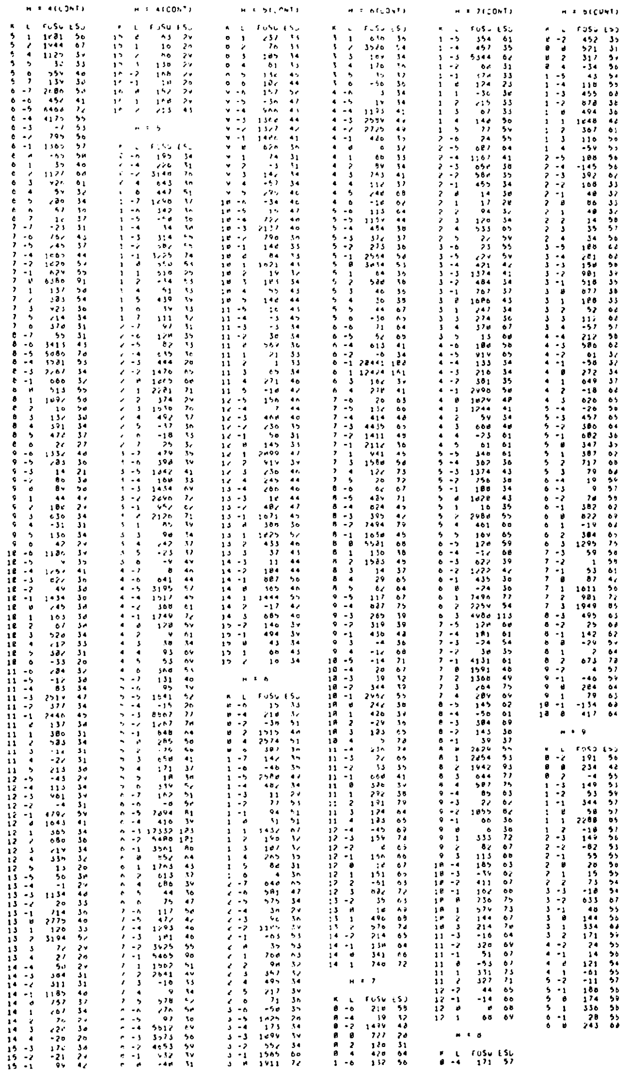

included at the measured value of $|F_o|^2$ including those with small negative values. In the preliminary refinement the least-squares weights were set at $1/\sigma_1^2(F_o^2)$ since the constant p was not known in advance. This weighting scheme placed too much emphasis on the strong reflexions, to the extent that the calculation diverged when the full parameter shifts were applied. Suitable acceleration factors (0·25 for positional parameters and 0·20 for thermal, scale and extinction parameters) were arrived at by trial and error. Then cycles of least-squares calculations reduced the residuals* $R(F)$ and $R(F^2)$ to 0·098 and 0·088, respectively, and the 'goodness-of-fit' index* G to 1·91.

The least-squares calculations were then continued with estimated absolute weighting factors, the constant p being determined from the results of an analysis of structure-factor agreement in the manner described in the TABX paper. This gave a value of 0·0043 for p. Six cycles of refinement, full shifts being applied, were performed with the absolute weights, and these reduced all parameter shifts to insignificant values. The final residuals were 0·093 and 0·087, and the final G index was 1·12. The extinction parameters r_1^* and r_2^* were 0·145 (39) × 10^{-4} cm and 0·100 (13) × 10^{-4} cm, respectively.

The positional and thermal parameters for the refined model are listed in Table 4.

Discussion

Molecular structure

The TAB molecule is shown in Fig. 1 viewed normal to the plane of the benzene ring. The interatomic distances and angles involving bonded atoms, and the non-bonded distances between neighbouring terminal

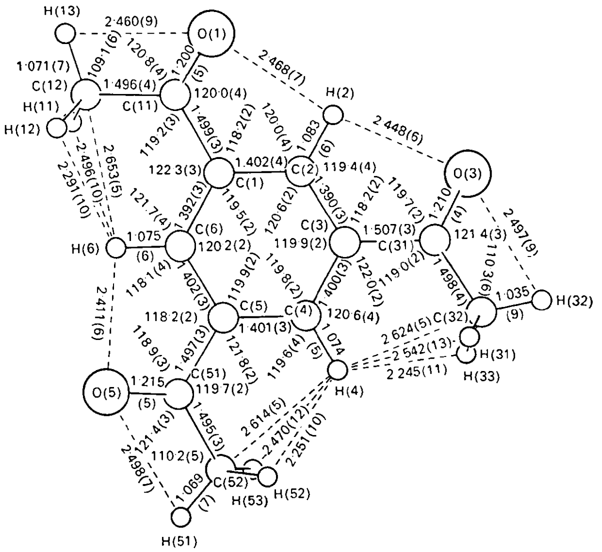

Fig. 1. Intramolecular distances (Å) and angles (°) with model viewed normal to the plane of the ring.

Table 4. *Final fractional coordinates and anisotropic thermal parameters* (× 10^4)

The e.s.d.'s, which are enclosed in parentheses, correspond to the least significant digits in each case. The thermal parameters are defined for a temperature factor of the form $\exp[-(b_{11}h^2+b_{12}hk+b_{22}k^2+b_{13}hl+b_{23}kl+b_{33}l^2)]$.

	x	y	z	b_{11}	b_{12}	b_{22}	b_{13}	b_{23}	b_{33}
C(1)	3363 (3)	3700 (2)	2905 (3)	105 (4)	12 (3)	22 (1)	61 (7)	0 (3)	205 (5)
C(2)	4891 (3)	3765 (2)	2274 (3)	107 (4)	22 (3)	25 (1)	59 (7)	5 (4)	204 (5)
C(3)	5617 (3)	4526 (2)	2131 (3)	88 (4)	16 (3)	26 (1)	63 (7)	4 (3)	166 (5)
C(4)	4818 (3)	5235 (2)	2618 (3)	88 (4)	8 (3)	25 (1)	28 (6)	−2 (3)	150 (4)
C(5)	3288 (3)	5174 (2)	3244 (3)	85 (4)	7 (7)	23 (1)	46 (6)	0 (3)	155 (5)
C(6)	2563 (3)	4405 (2)	3378 (3)	98 (4)	8 (9)	23 (1)	46 (7)	0 (3)	185 (5)
C(11)	2641 (4)	2864 (2)	3028 (5)	127 (5)	9 (4)	23 (1)	126 (9)	2 (4)	316 (7)
C(31)	7266 (3)	4555 (2)	1458 (4)	98 (4)	25 (3)	32 (1)	89 (7)	3 (4)	182 (5)
C(51)	2386 (4)	5914 (2)	3784 (4)	93 (4)	7 (3)	24 (1)	68 (7)	−14 (3)	198 (5)
C(12)	918 (4)	2787 (2)	3401 (6)	134 (5)	−16 (4)	31 (1)	151 (11)	−27 (5)	416 (10)
C(32)	8160 (4)	5350 (2)	1530 (5)	119 (5)	−5 (4)	40 (1)	122 (13)	−4 (4)	251 (7)
C(52)	3008 (6)	6749 (2)	3412 (5)	135 (5)	8 (5)	23 (1;	89 (10)	−5 (4)	309 (7)
O(1)	3435 (5)	2268 (2)	2793 (8)	192 (8)	17 (5)	24 (2)	393 (23)	2 (8)	834 (24)
O(3)	7843 (5)	3941 (3)	878 (6)	153 (6)	33 (4)	40 (2)	181 (12)	−24 (5)	301 (9)
O(5)	1156 (5)	5818 (2)	4516 (7)	140 (5)	−3 (4)	33 (2)	232 (13)	−41 (6)	414 (11)
H(2)	5523 (8)	3220 (4)	1909 (11)	180 (10)	35 (7)	34 (2)	133 (20)	−30 (9)	363 (16)
H(4)	5364 (7)	5826 (3)	2508 (9)	143 (9)	0 (7)	33 (2)	107 (18)	2 (8)	306 (14)
H(6)	1391 (7)	4380 (3)	3868 (9)	144 (8)	5 (7)	33 (2)	126 (18)	−3 (8)	318 (33)
H(11)	197 (10)	3109 (6)	2526 (21)	170 (12)	−2 (13)	76 (4)	−30 (35)	24 (21)	652 (69)
H(12)	684 (11)	3074 (5)	4588 (14)	273 (15)	−64 (13)	74 (4)	405 (33)	−52 (16)	516 (25)
H(13)	605 (10)	2151 (4)	3432 (19)	223 (13)	−32 (9)	38 (3)	324 (38)	−23 (15)	847 (43)
H(31)	8356 (15)	5558 (7)	2782 (15)	468 (26)	−261 (22)	102 (6)	231 (42)	−123 (19)	401 (23)
H(32)	9240 (10)	5292 (6)	956 (17)	205 (13)	−40 (12)	75 (12)	389 (36)	−67 (18)	666 (35)
H(33)	7477 (10)	5815 (5)	847 (17)	249 (12)	−21 (12)	60 (12)	46 (34)	175 (18)	708 (35)
H(51)	2240 (9)	7206 (4)	3904 (14)	218 (8)	16 (16)	38 (8)	269 (28)	−42 (11)	596 (25)
H(52)	4186 (9)	6824 (4)	3994 (16)	183 (9)	−51 (9)	48 (9)	−27 (29)	−3 (14)	680 (32)
H(53)	3165 (16)	6830 (5)	2141 (14)	553 (14)	−52 (14)	49 (14)	255 (41)	58 (12)	397 (22)

---

* $R(F)=\sum(F_o-F_c)/\sum F_o$, $R(F^2)=\sum(F_o^2-F_c^2)/\sum F_o^2$, $G=[\sum w(F_o^2-F_c^2)^2/(m-n)]^{1/2}$.

atoms, are indicated. It should be noted that corrections for thermal motion effects have not been applied. Those bond lengths and angles involving hydrogen which are not shown on Fig. 1 are given in Table 5.

Table 5. *Bond distances and angles involving hydrogen*

The remaining hydrogen distances and angles are shown on Fig. 1.

C(12)–H(11)	1·019 (11) Å
C(12)–H(12)	1·051 (11)
C(11)–C(12)–H(11)	111·8 (6)°
C(11)–C(12)–H(12)	112·3 (6)
H(11)–C(12)–H(12)	101·5 (8)
H(11)–C(12)–H(13)	112·3 (8)
H(12)–C(12)–H(13)	110·7 (8)
C(32)–H(31)	1·019 (11) Å
C(32)–H(33)	1·068 (10)
C(31)–C(32)–H(31)	112·0 (7)°
C(31)–C(32)–H(33)	110·3 (6)
H(31)–C(32)–H(32)	109·6 (9)
H(31)–C(32)–H(33)	105·7 (9)
H(32)–C(32)–H(33)	108·3 (8)
C(52)–H(52)	1·064 (9) Å
C(52)–H(53)	1·000 (11)
C(51)–C(52)–H(52)	110·5 (6)°
C(51)–C(52)–H(53)	112·0 (7)
H(51)–C(52)–H(52)	109·7 (7)
H(51)–C(52)–H(53)	111·8 (8)
H(52)–C(52)–H(53)	102·4 (8)

The extent of pseudosymmetry associated with the molecule is of particular interest. The highest point-group symmetry possible for the molecule is 3*m*. While it can be said that the molecule approximates to this description, the disposition of the oxygen atoms and methyl groups breaks the threefold symmetry axis so that there are two pseudo-mirror planes normal to the plane of the ring and coincident with the bonds C(1)–C(4) and C(2)–C(5). This arrangement appears to have been adopted in order to minimize the number of intermolecular van der Waals contacts between methyl groups (see below).

Another feature of the molecule is the deviation of the oxygen and methyl carbon atoms from the central plane of the molecule as can be seen from the analysis of planarity summarized in Table 6. The non-hydrogen atoms of the acetyl group, together with the ring carbon to which the group is bonded, form a planar array inclined to the central plane of the molecule. Each group is therefore twisted about the C(sp^2,ring)–C(sp^2,acetyl) bond, giving the molecule a slight propeller-like appearance, similar to that observed in 1,3,5-triphenylbenzene (Lonsdale, 1937), with torsion angles of 9·4, 8·2 and 8·9° for the groups bonded to C(1), C(3) and C(5), respectively. It is apparent that the rotation is due to intramolecular repulsive forces as the effect gives increased distances for contacts of the type C(12)···H(6) and O(1)···H(2). However a detailed analysis of these interactions is not feasible in view of the paucity of information in the literature on intramolecular van der Waals radii.

It is interesting to note that all three acetyl groups have a hydrogen atom residing within the group plane. The effect is probably due to either or both of the following interactions. First, there is the possibility of attraction between neighbouring oxygen and hydrogen atoms, and this is supported by the additional observation that each acetyl group bends slightly (*ca.* 2°) towards the ring hydrogen atom situated adjacent to the oxygen. The second type of interaction to which the orientation of the methyl hydrogen atoms might be attributed is repulsion between the methyl and ring hydrogen atoms. This latter point is quite conceivable

Table 6. *Least-squares planes for the central portion of the molecule and acetyl groups*

The coefficients *A*, *B*, *C*, and *D* are defined such that $Ax+By+Cz+D=0$. In the list of displacements from each plane the most significant figures of the positional standard deviations are enclosed in parentheses.

Coefficients		Displacements	
A	0·3462	C(1)	0·003 (5) Å
B	−0·0903	C(2)	−0·002 (5)
C	0·9338	C(3)	−0·003 (5)
D	−2·447	C(4)	−0·001 (5)
		C(5)	−0·001 (5)
		C(6)	−0·005 (5)
		C(11)	0·002 (6)
		C(31)	0·003 (5)
		C(51)	0·004 (5)
		H(2)	0·01 (1)
		H(4)	−0·01 (1)
		H(6)	−0·00 (1)
		C(12)	−0·228 (6)
		O(1)	0·157 (8)
		C(32)	0·196 (6)
		O(3)	−0·142 (8)
		C(52)	−0·198 (7)
		O(5)	0·170 (7)

Coefficients		Displacements	
A	0·1999	C(1)	−0·002 (6) Å
B	−0·0298	C(11)	0·008 (6)
C	0·9794	C(12)	−0·002 (6)
D	−2·528	O(1)	−0·003 (8)
		H(11)	−0·78 (2)
		H(12)	0·82 (2)
		H(13)	−0·00 (2)
A	0·3375	C(3)	0·000 (5)
B	−0·2317	C(31)	−0·001 (5)
C	0·9124	C(32)	0·000 (6)
D	−1·324	O(3)	0·000 (8)
		H(31)	0·82 (2)
		H(32)	−0·06 (2)
		H(33)	−0·83 (2)
A	0·4645	C(5)	0·000 (5)
B	−0·0003	C(51)	0·001 (5)
C	0·8856	C(52)	0·000 (7)
D	−3·396	O(5)	0·000 (7)
		H(51)	0·02 (2)
		H(52)	0·84 (2)
		H(53)	−0·77 (2)

in view of similar effects observed in various overcrowded molecules.

The bonded interatomic distances and associated angles agree satisfactorily with values given in the literature for covalent bonds in similar environments to those found in TAB. It is unfortunate that there is very little available in the literature describing the geometry of the acetyl group. A pleasing feature of the results is the agreement between the chemically-equivalent distances (see Table 7), thus confirming the reliability of the error estimates quoted for the positional parameters.

Table 7. *Bond distances (in Å) for the final least-squares positions, uncorrected for librational effects*

The e.s.d.'s (enclosed in parentheses) are quoted for the least significant digits.

		Mean
C(1)–C(2)	1·402 (4)	1·398 (2)
C(2)–C(3)	1·390 (3)	
C(3)–C(4)	1·400 (3)	
C(4)–C(5)	1·401 (3)	
C(5)–C(6)	1·402 (3)	
C(6)–C(1)	1·392 (3)	
C(1)–C(11)	1·499 (3)	1·501 (2)
C(3)–C(31)	1·507 (3)	
C(5)–C(51)	1·497 (3)	
C(11)–C(12)	1·496 (4)	1·496 (2)
C(31)–C(32)	1·498 (4)	
C(51)–C(52)	1·495 (3)	
C(11)–O(1)	1·200 (5)	1·208 (3)
C(31)–O(3)	1·210 (4)	
C(51)–O(5)	1·215 (5)	
C(2)–H(2)	1·083 (6)	1·077 (3)
C(4)–H(4)	1·074 (5)	
C(6)–H(6)	1·075 (6)	
C(12)–H(11)	1·019 (11)	1·044 (3)
C(12)–H(12)	1·051 (11)	
C(12)–H(13)	1·071 (7)	
C(32)–H(31)	1·019 (11)	
C(32)–H(32)	1·035 (9)	
C(32)–H(33)	1·068 (10)	
C(52)–H(51)	1·069 (8)	
C(52)–H(52)	1·064 (9)	
C(52)–H(53)	1·000 (11)	

Molecular packing

The crystal structure is shown in Fig. 2 in a view down **c***. The molecules are bonded into layers separated by approximately $c/4$. Within the layers the molecules are linked by van der Waals attraction through contacts of the type O···CH_3 and CH_3···CH_3. The predominance of the former type facilitates higher packing efficiency.

A complete list of intermolecular distances is given in Table 8. Contacts have been included if the appropriate distance does not exceed the sum of the van der Waals radii (Pauling, 1960) by more than 0·2 Å. Note that for O···H–C contacts the data are tabulated if either O···H or O···C satisfies the criterion. A similar procedure has been adopted in accepting C–H···H–C contacts according to either the H···H or C···C distances. A feature of interest is that the acetyl groups bonded to C(1) and C(5) form most of the close contacts. This may well explain why the group bonded to C(3) has the least pronounced thermal motion of the three groups.

Table 8. *Intermolecular close contacts* (Å)

The criteria used to accept contacts for inclusion in the table are given in the text.

O···C contacts		O···H	O···C
O(1)···	$\mathrm{H}(4^{iv})$–$\mathrm{C}(4^{iv})$	2·58	3·65
	$\mathrm{H}(33^{iv})$–$\mathrm{C}(32^{iv})$	2·72	3·46
	$\mathrm{H}(52^{iv})$–$\mathrm{C}(52^{iv})$	2·59	3·29
O(3)···	$\mathrm{H}(11^{v})$–$\mathrm{C}(12^{v})$	2·65	3·64
O(5)···	$\mathrm{H}(31^{ii})$–$\mathrm{C}(32^{ii})$	2·65	3·37
	$\mathrm{H}(6^{ii'})$–$\mathrm{C}(6^{ii'})$	2·56	3·62
	$\mathrm{H}(12^{ii''})$–$\mathrm{C}(12^{ii''})$	2·50	3·33

C···C contacts	C···C	H···H
C(2)–H(2)···$\mathrm{H}(52^{iv})$–$\mathrm{C}(52^{iv})$	3·79	2·40
$\mathrm{C}(32^{ii})$–$\mathrm{H}(32^{ii})$···$\mathrm{H}(32^{i'})$–$\mathrm{C}(32^{i'})$	4·19	2·22
C(12)–H(11)···$\mathrm{H}(51^{iii})$–$\mathrm{C}(52^{iii})$	3·88	2·69
C(3)···$\mathrm{C}(51^{i''})$	3·52	–
C(4)···$\mathrm{C}(5^{i''})$	3·51	–
C(4)···$\mathrm{C}(31^{i'})$	3·49	–

Rigid-body motion

The procedure adopted in analysing the rigid-body motion of the molecule was the TLX method proposed

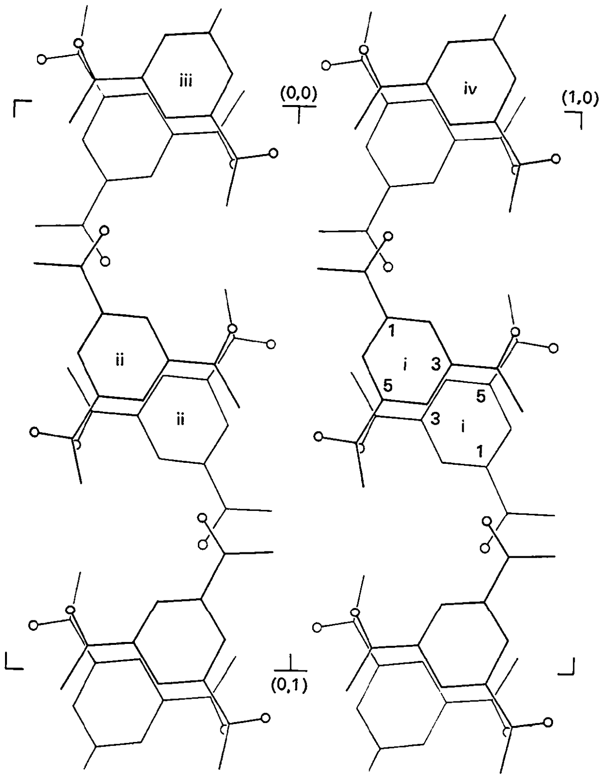

Fig. 2. Packing diagram as viewed down **c***. The equivalent position symbols are defined in Table 8.

Table 8 (*cont.*)

Equivalent position notation

Without superscript	(x, y, z)*	i′ $(1-x, 1-y, -z)$	i″ $(1-x, 1-y, 1-z)$
ii	$(-1+x, y, z)$	ii′ $(-x, 1-y, -z)$	ii″ $(-x, 1-y, 1-z)$
iii	$(-x, -\frac{1}{2}+y, \frac{1}{2}-z)$		
iv	$(1-x, -\frac{1}{2}+y, \frac{1}{2}+z)$		

* Position i in Fig. 2.

by Pawley (1963, 1970) which uses iterative least-squares calculations to fit the translational and librational tensors **T** and **L**, and the origin of **L**, to the final set of atomic **U** tensors. The calculation was first performed for all atoms in the molecule. As might be expected this gave extremely poor agreement between the calculated and observed **U** tensors, due no doubt to the complexity of the modes associated with the acetyl groups. A subsequent analysis involving only the nine central carbon atoms and the ring hydrogen atoms improved the level of agreement, although the hydrogens did show excess motion which can be attributed to stretching and bending modes. The final calculations, for which the results are reported in Tables 9–11, were therefore conducted with zero weights assigned to the ring hydrogens. Agreement between the calculated and observed **U** tensors is satisfactory for the nine central carbons. The preferred rigid-body vibration is normal to the plane of the molecule and the preferred libration axis lies close to molecular axis **1**.

Table 9. *Rigid-body* **T** *and* **L** *elements referred to the molecular axes*

Axis **1** is directed along the direction C(6)–C(3); axis **2** is along the direction C(1)–C(5); axis 3 is perpendicular to the molecular plane.

$$\mathbf{T}=\begin{bmatrix} 307 & & \\ 38 & 310 & \\ -19 & 30 & 458 \end{bmatrix} (\text{Å}^2\times10^4)$$

$$\mathbf{L}=\begin{bmatrix} 14\cdot8 & & \\ -0\cdot7 & 3\cdot0 & \\ 1\cdot0 & -0\cdot7 & 3\cdot0 \end{bmatrix} (\text{deg}^2)$$

Origin of **L** axes in the molecular axial system,

$-0\cdot28$, $0\cdot38$, $-0\cdot13$ Å.

Table 10. *R.m.s. values for the principal axes of the* **T** *and* **L** *tensors referred to the system of molecular axes*

Tensor	R.m.s. value	Direction cosines relative to molecular axes Axis 1	Axis 2	Axis 3
T	0·22 Å	−0·076	0·169	0·983
	0·19	0·712	0·700	−0·065
	0·16	0·698	−0·694	0·174
L	3·8°	0·995	−0·053	0·088
	1·9	−0·101	0·669	0·736
	1·5	−0·020	0·741	0·671

A more detailed analysis of the thermal motion is being conducted in this laboratory.

The investigation was sponsored by the Australian Institute of Nuclear Science and Engineering. One of us (B.H.O'C.) held a Queen Elizabeth Fellowship during the course of the investigation. We are both obliged to Dr E. N. Maslen for his close interest in the work.

References

Bacon, G. E. (1962). *Neutron Diffraction*, p. 61. Oxford: Clarendon Press.

Busing, W. R. & Levy, H . A. (1957). *Acta Cryst.* **10**, 180–182.

Coppens, P. (1967). *Science*, **158**, 1577–1579.

Coppens, P., Sabine, T. M., Delaplane, R. G. & Ibers, J. A. (1969). *Acta Cryst.* B**25**, 2451–2458.

Coppens, P. & Vos, A. (1971). *Acta Cryst.* B**27**, 146–158.

Lonsdale, K. (1937). *Z. Kristallogr.* **97**, 91–94.

Melkonian, E. (1949). *Phys. Rev.* **76**, 1744–1759.

O'Connor, B. H. (1973). *Acta Cryst.* B**29**, 1893–1903.

Pauling, L. (1960). *The Chemical Bond*, p. 260. Ithaca: Cornell Univ. Press.

Pawley, G. S. (1963). *Acta Cryst.* **16**, 1204–1208.

Pawley, G. S. (1970). *Acta Cryst.* A**26**, 289–292.

Zachariasen, W. H. (1969). *Acta Cryst.* A**25**, 102.

Table 11. *The observed and calculated vibration components* ($\text{Å}^2\times10^3$) *referred to the molecular axial system*

	U_{11} obs	U_{11} cal	U_{12} obs	U_{12} cal	U_{22} obs	U_{22} cal	U_{13} obs	U_{13} cal	U_{23} obs	U_{23} cal	U_{33} obs	U_{33} cal
C(1)	36	33	3	3	30	31	−3	−3	4	4	61	57
C(2)	37	33	6	5	34	32	−3	−2	7	4	60	57
C(3)	29	31	4	4	35	34	−1	−1	4	3	51	49
C(4)	32	31	3	3	34	32	−3	−2	1	3	44	50
C(5)	29	31	2	4	31	31	−2	−2	2	2	46	49
C(6)	34	31	2	3	31	32	−4	−2	3	4	54	48
C(11)	40	39	2	1	31	32	−5	−5	8	6	96	86
C(31)	30	31	9	5	43	40	1	−2	5	5	57	55
C(51)	31	35	4	6	31	33	−4	−3	0	1	60	66
H(2)	60	37	14	7	44	33	−5	−3	2	4	111	75
H(4)	47	34	−1	1	45	33	−4	−4	5	3	92	63
H(6)	45	31	2	3	45	36	−4	−2	5	4	97	51